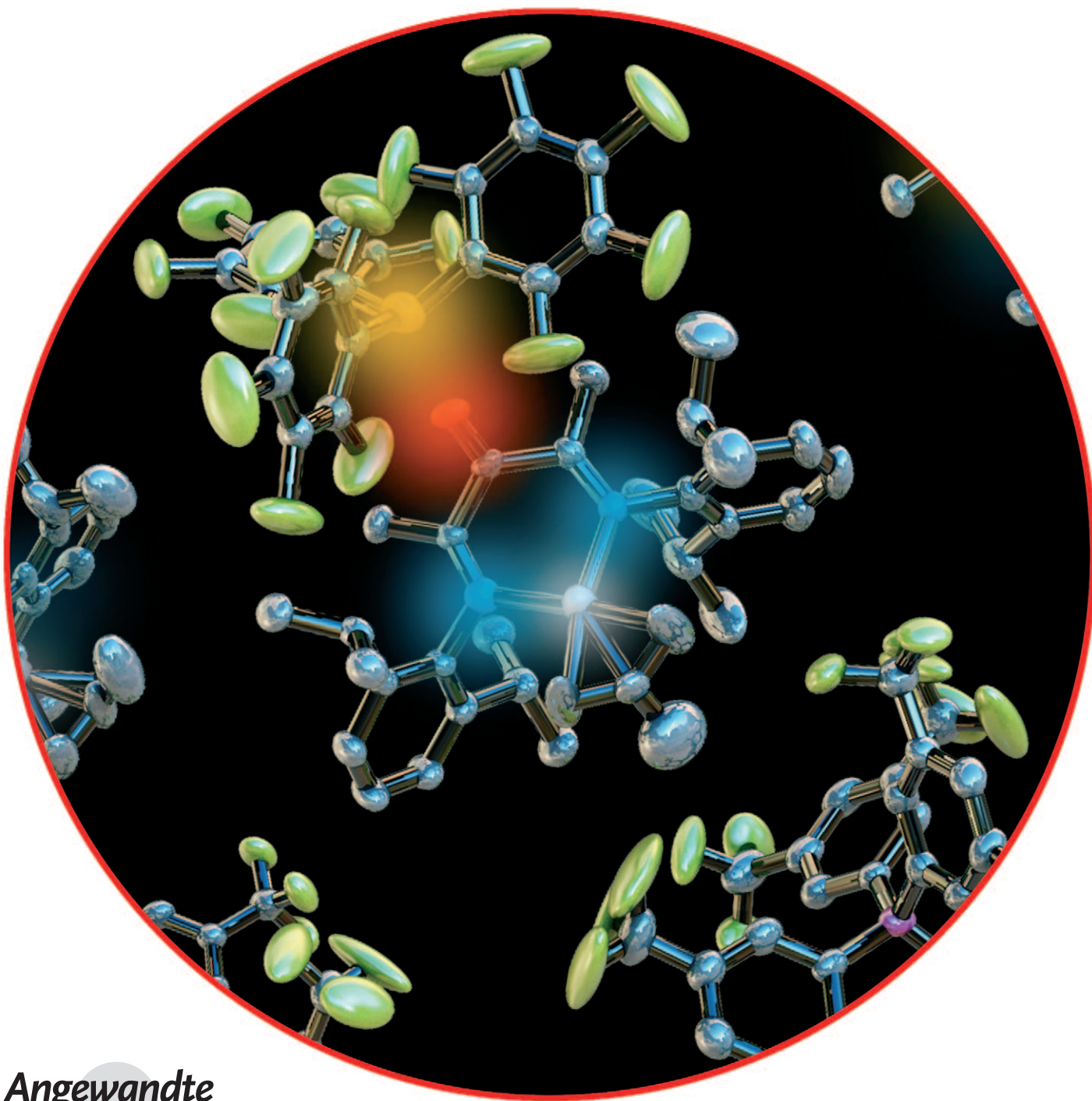


# Well-Defined Cationic Methallyl $\alpha$ -Keto- $\beta$ -Diimine Complexes of Nickel\*\*

Jason D. Azoulay, Zachary A. Koretz, Guang Wu, and Guillermo C. Bazan\*



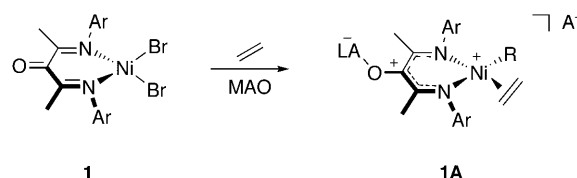
Angewandte  
Chemie

Polyolefins are a range of commodity materials with major economic implications.<sup>[1]</sup> Despite a significant historical record, the requirement of efficient methods for their preparation and the search for new macromolecular architectures continue to drive the development and design of homogeneous transition-metal complexes in both academic and industrial laboratories. Late-transition-metal systems are less oxophilic than their early-transition-metal counterparts.<sup>[1]</sup> They have been shown to participate in “chain-walking” reactions,<sup>[2]</sup> exhibit living behavior,<sup>[3]</sup> incorporate and tolerate polar functionalities,<sup>[1,4]</sup> and have been used in water.<sup>[5]</sup> Such flexibility in reactivity is relevant for the development of new materials.<sup>[1g,6]</sup>

Cationic catalysts and/or initiators are typically generated by electrophilic abstraction reactions from neutral complexes by using coactivators, such as methylaluminoxane (MAO).<sup>[2b,7]</sup> The activated complex is in most cases an ion-paired species consisting of an electrophilic transition-metal cation and a bulky noncoordinating counterion. Other methods of activation have also been reported. More specifically, complexes containing  $\alpha$ -iminocarboxamidato and related ligands can be activated by the binding of Lewis acids to lone pairs of electrons on functional groups within the ligand framework.<sup>[6b,8]</sup> Such a process leads to the formation of zwitterionic complexes, enables activation at a site removed from the monomer-insertion trajectory, and results in a net withdrawal of electron density from the metal atom.<sup>[8]</sup>

The molecular requirements for the two activation processes described above led to the design of compound **1** (Scheme 1), in which a nickel center is coordinated by a bulky  $\alpha$ -keto- $\beta$ -diimine ligand. Active sites are generated by using trimethylaluminum (TMA), MAO, and modified MAO (MMAO) coactivators.<sup>[9,10]</sup> The presence of the carbonyl functionality on the ligand framework leads to an increase in the rate of polyethylene (PE) production by two orders of magnitude relative to that observed with a nearly isostructural  $\beta$ -diimine analogue.<sup>[11]</sup> This increased activity has been attributed to the formation of a cationic species in which the metal center is further depleted of electron density by the attachment of a Lewis acid at the carbonyl site, as in **1A**. Living-polymerization characteristics can be attained by reducing the TMA content in MAO through the removal of volatile species.<sup>[3c]</sup>

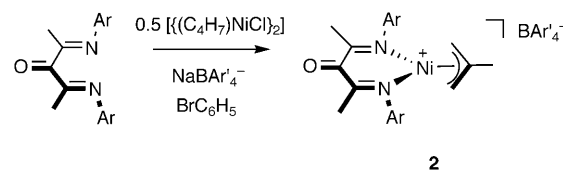
The formation of **1A** and the responsibility of this species for promoting the polymerization reactions have not been fully verified. Commercially available MAO and MMAO are complex mixtures of oligomers containing various weight



**Scheme 1.** Proposed active site upon activation with MAO. R = alkyl, A<sup>−</sup> = charge-compensating counterion, Ar = 2,6-diisopropylphenyl.

ratios of alkyl aluminum species.<sup>[12]</sup> Furthermore, the excess aluminum (Al/Ni 250:1) required to activate **1** complicates the in situ observation and characterization of initiating/propagating sites. In response to these challenges, we report the synthesis and characterization of a discrete, cationic nickel analogue of **1**: [2,4-bis(2,6-diisopropylphenylimino)pentan-3-one- $\kappa^2$ N,N']Ni( $\eta^3$ -C<sub>4</sub>H<sub>7</sub>)<sup>+</sup>BAR'<sub>4</sub><sup>−</sup> (**2**, Ar' = 3,5-(CF<sub>3</sub>)<sub>2</sub>C<sub>6</sub>H<sub>3</sub>). We found evidence for increased polymerization rates upon the binding of a Lewis acid to the carbonyl functionality. Additionally, we disclose new reactivity with alkyl aluminum compounds that is relevant for understanding the experimental conditions required to achieve living polymerization.

Complex **2** was synthesized in 78% yield by the reaction of 2,4-bis(2,6-diisopropylphenylimino)pentan-3-one with [(C<sub>4</sub>H<sub>7</sub>)NiCl]<sub>2</sub> in the presence of NaBAR'<sub>4</sub><sup>−</sup> (Scheme 2). In contrast to the paramagnetic analogue **1**, complex **2** is



**Scheme 2.** Synthesis of **2**. Ar = 2,6-diisopropylphenyl, Ar' = 3,5-(CF<sub>3</sub>)<sub>2</sub>C<sub>6</sub>H<sub>3</sub>.

diamagnetic. Two resonances were observed in the <sup>1</sup>H NMR spectrum of **2** in CD<sub>2</sub>Cl<sub>2</sub> for the *syn* and *anti* allylic hydrogen atoms: singlets at  $\delta$  = 2.30 (H<sub>anti</sub>) and 2.20 ppm (H<sub>syn</sub>). The presence of these resonances indicates the structural rigidity of the  $\pi$ -allyl ligand on the NMR time scale.<sup>[13]</sup> In the <sup>13</sup>C NMR spectrum, the CH<sub>2</sub> carbon atoms appear as a singlet at  $\delta$  = 66.0 ppm, the imine carbon atoms at  $\delta$  = 175.5 ppm, and the carbonyl carbon atom at  $\delta$  = 183.6 ppm; these signals indicate that the ligand is bound in an N,N' fashion. The <sup>11</sup>B and <sup>19</sup>F NMR spectra show characteristic singlets for the BAR'<sub>4</sub><sup>−</sup> counterion at  $\delta$  = −6.7 and −64.2 ppm, respectively. A single-crystal X-ray diffraction study confirmed the identity of the complex (Figure 1). A distorted square-planar geometry around the nickel center was observed, whereby the six-membered chelate adopts a boatlike conformation similar to that in **1**.<sup>[9]</sup> The 2,6-diisopropyl groups project toward the axial sites of the cation in a configuration that was anticipated to retard the rate of chain transfer and lead to the formation of high-molecular-weight polymers.<sup>[7a]</sup>

Interactions with different Lewis acidic aluminum compounds were first probed by examination of the reaction of **2** with Al(C<sub>6</sub>F<sub>5</sub>)<sub>3</sub>·(C<sub>7</sub>H<sub>8</sub>)<sub>0.5</sub> (1 equiv).<sup>[14]</sup> A new organometallic

[\*] J. D. Azoulay, Z. A. Koretz, G. Wu, Prof. Dr. G. C. Bazan  
Mitsubishi Chemical Center for Advanced Materials  
Center for Polymers and Organic Solids  
Departments of Chemistry & Biochemistry and Materials  
The University of California, Santa Barbara, CA 93106 (USA)  
Fax: (+1) 805-893-4120  
E-mail: bazan@chem.ucsb.edu

[\*\*] We are grateful to the Department of Energy BES and the Mitsubishi Chemical Center for Advanced Materials for support of this research.

Supporting information for this article is available on the WWW under <http://dx.doi.org/10.1002/anie.201003125>.

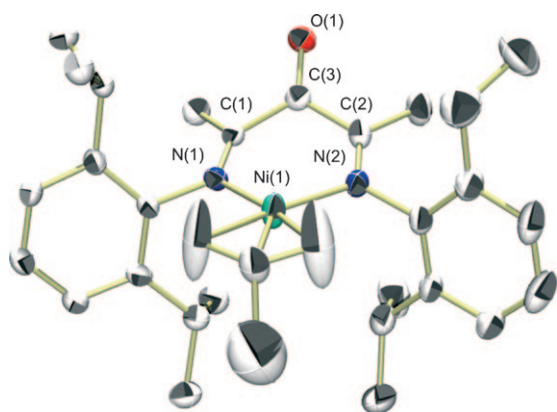
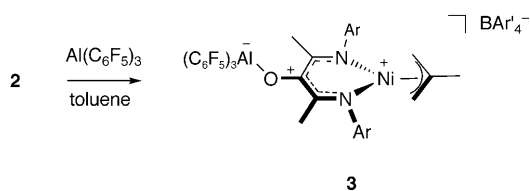


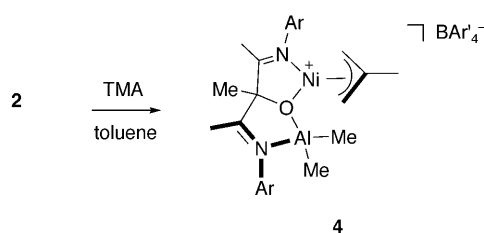
**Figure 1.** ORTEP drawing of the cation in **2**.<sup>[19]</sup> Hydrogen atoms and the  $\text{BAR}_4^-$  counterion have been omitted for clarity. Thermal ellipsoids are drawn at 35% probability. Selected bond lengths [Å] and angles [°]: C(2)–N(2) 1.279(6), C(2)–C(3) 1.515(7), C(1)–N(1) 1.272(6), C(1)–C(3) 1.527(7), C(3)–O(1) 1.203(6), Ni(1)–N(1) 1.947(4), Ni(1)–N(2) 1.946(4), Ni(1)–C(5) 1.995(6); N(1)–C(1)–C(3) 118.6(5), C(1)–C(3)–C(2) 122.4(5), N(2)–C(2)–C(3) 119.6(5), C(2)–N(2)–Ni(1) 123.0(4), N(1)–Ni(1)–N(2) 96.37(18), Ni(1)–N(1)–C(1) 123.9(4).

product formed within minutes, as determined by  $^1\text{H}$  NMR spectroscopy in  $\text{C}_6\text{D}_6$  or  $\text{CD}_2\text{Cl}_2$  (in which the compound is unstable after 1 h). For example, in  $\text{CD}_2\text{Cl}_2$ , the resonances for the allylic protons appeared at  $\delta = 2.38$  ( $H_{\text{anti}}$ ) and 2.30 ppm ( $H_{\text{syn}}$ ). The downfield shift of these signals relative to those of **2** is indicative of a more electrophilic metal center. Characteristic resonances observed in the  $^{19}\text{F}$  NMR spectrum ( $\text{C}_6\text{D}_6$ ) at  $\delta_{\text{F}} = -139$  (6F, *ortho*),  $-154$  (3F, *para*), and  $-162$  ppm (6F, *meta*) are consistent with carbonyl coordination to aluminum.<sup>[15]</sup> A downfield shift in the  $^{13}\text{C}$  NMR spectrum in  $\text{C}_6\text{D}_6$  indicated a more polarized C=O bond in the product relative to that in **2** ( $\Delta\delta_{\text{CO}} = 16.1$  ppm; see the Supporting Information). These observations are consistent with the formation of **3** (Scheme 3). Single crystals of **3** were not obtained despite repeated attempts owing to the lack of crystallinity in this complex. The carbonyl stretching frequency in the IR (KBr) spectrum of **3** occurs at a lower frequency in comparison to that observed for **2** ( $\Delta\nu_{\text{CO}} = -52\text{ cm}^{-1}$ ), as would be expected for the decreased C=O bond order upon activation.

The reaction of **2** with TMA (1 equiv) resulted in the formation of **4** (Scheme 4). The  $^1\text{H}$  and  $^{13}\text{C}$  NMR spectra of **4** are consistent with the formation of a mixture of diastereomers in a 1.4:1 ratio. Four peaks corresponding to the methyl groups attached to aluminum were observed between  $\delta = -0.50$  and  $-0.72$  ppm. Single crystals of **4** suitable for X-ray



**Scheme 3.** Reaction of **2** with  $\text{Al}(\text{C}_6\text{F}_5)_3$  to form **3**. Ar = 2,6-diisopropylphenyl, Ar' = 3,5-( $\text{CF}_3$ ) $_2\text{C}_6\text{H}_3$ .



**Scheme 4.** Reaction of **2** with TMA. Reaction conditions:  $\text{AlMe}_3$  (1 equiv), toluene,  $-35^\circ\text{C} \rightarrow \text{RT}$ . Ar = 2,6-diisopropylphenyl, Ar' = 3,5-( $\text{CF}_3$ ) $_2\text{C}_6\text{H}_3$ .

crystallography were obtained at  $-35^\circ\text{C}$  from a toluene solution. The results of the structural characterization of **4** are shown in Figure 2. The addition of TMA in toluene to **2** resulted in alkylation of the exocyclic carbonyl group and rearrangement of the ligand framework. This reaction led to a

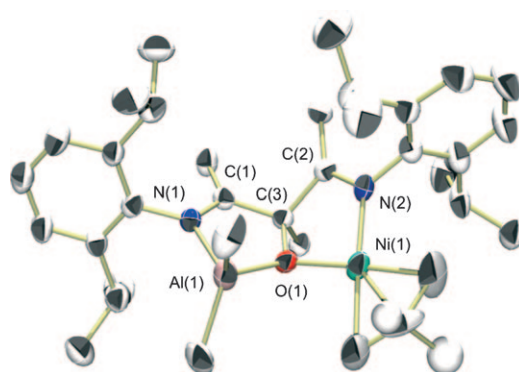
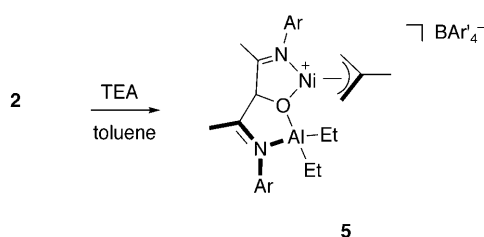


**Figure 2.** ORTEP drawing of the cation in **4**.<sup>[19]</sup> Hydrogen atoms and the  $\text{BAR}_4^-$  counterion have been omitted for clarity. Thermal ellipsoids are drawn at 35% probability. Selected bond lengths [Å] and angles [°]: Ni(1)–N(2) 1.904(6), N(2)–C(2) 1.267(8), C(2)–C(3) 1.546(9), C(3)–O(1) 1.407(7), O(1)–Ni(1) 1.904(5), C(3)–C(1) 1.538(9), O(1)–Al(1) 1.806(5), Al(1)–N(1) 1.972(6), N(1)–C(1) 1.278(7); Ni(1)–N(2)–C(2) 118.1(5), N(2)–C(2)–C(3) 112.3(6), C(2)–C(3)–O(1) 107.9(5), C(3)–O(1)–Ni(1) 112.8(4), O(1)–Ni(1)–N(2) 104.90, C(3)–O(1)–Al(1) 118.66, O(1)–Al(1)–N(1) 82.7(2), Al(1)–N(1)–C(1) 114.3(5), N(1)–C(1)–C(3) 115.1(6), C(1)–C(3)–O(1) 107.7(5).

binuclear organometallic species in which nickel and aluminum are ligated in an N,O,N' fashion with the oxygen atom bridging the aluminum and nickel centers. The nickel atom in this complex adopts a distorted square-planar geometry with a planar five-membered N(2),O chelate. The 2,6-diisopropyl substituents on the aryl group bound to N(2) project toward the axial positions of the nickel coordination plane. Aluminum is N,O-bound with a tetrahedral arrangement of ligands.

The reaction of **2** with triethylaluminum (TEA) yielded a distinct organometallic product. Specifically, the addition of TEA (1 equiv) to **2** resulted in the quantitative formation of complex **5** (Scheme 5). The molecular structure of **5** (Figure 3) was determined by single-crystal studies. The characterization of **5** by NMR spectroscopy in solution was consistent with this structure (see the Supporting Information). Interestingly, although compounds **4** and **5** have structural similarities, and alkylation reactions with TMA





**Scheme 5.** Reaction of **2** with TEA. Reaction conditions:  $\text{AlEt}_3$  (1 equiv), toluene,  $-35^\circ\text{C} \rightarrow \text{RT}$ . Ar = 2,6-diisopropylphenyl, Ar' = 3,5-( $\text{CF}_3$ ) $_2\text{C}_6\text{H}_3$ .

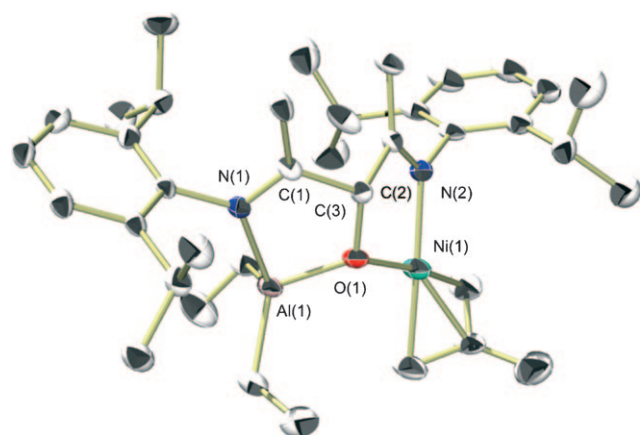


**Figure 3.** ORTEP drawing of the cation in **5**.<sup>[19]</sup> Hydrogen atoms and the  $\text{BAR}'_4^-$  counterion have been omitted for clarity. Thermal ellipsoids are drawn at 35% probability. Selected bond lengths [Å] and angles [°]: Ni(1)–N(2) 1.924(3), N(2)–C(2) 1.282(5), C(2)–C(3) 1.536(5), C(3)–O(1) 1.422(5), O(1)–Ni(1) 1.918(3), C(3)–C(1) 1.513(6), O(1)–Al(1) 1.829(3), Al(1)–N(1) 1.999(4), N(1)–C(1) 1.296(5); Ni(1)–N(2)–C(2) 116.8(3), N(2)–C(2)–C(3) 114.0(4), C(2)–C(3)–O(1) 108.5(3), C(3)–O(1)–Ni(1) 112.7(2), O(1)–Ni(1)–N(2) 83.05, C(3)–O(1)–Al(1) 118.12, O(1)–Al(1)–N(1) 83.0(4), Al(1)–N(1)–C(1) 113.7(3), N(1)–C(1)–C(3) 115.7(4), C(1)–C(3)–O(1) 108.4(3).

are well-established,<sup>[16]</sup> the reaction with TEA and subsequent formation of complex **5** proceeds with the elimination of ethylene, as evidenced by the  $^1\text{H}$  NMR spectrum ( $\delta = 5.4$  ppm in  $\text{CD}_2\text{Cl}_2$  at 210 K), probably through direct  $\beta$ -hydrogen transfer to the coordinated carbonyl group.<sup>[16,17]</sup> Comparison of the structural features of **4** and **5** shows that the bulkier ethyl groups in **5** result in a more crowded coordination plane at the nickel center (Figures 2 and 3).

We carried out a series of ethylene-polymerization test reactions with **2–5** under various conditions (Table 1). Compound **2** could initiate ethylene polymerization in the absence of a coactivator (Table 1, entries 1 and 2). Thus, the exposure of **2** to ethylene (500 psig) at  $50^\circ\text{C}$  resulted in the formation of crystalline low-molec-

ular-weight PE ( $T_m = 128^\circ\text{C}$ ) in low yield (Table 1, entry 1). The addition of ethylene to a solution of **2** in  $\text{CD}_2\text{Cl}_2$  in an NMR tube resulted in the consumption of the monomer and the appearance of a singlet corresponding to  $-(\text{CH}_2)_n-$  at  $\delta = 1.28$  ppm along with the formation of a white precipitate. That there is no large difference in the integration of signals attributed to **2** suggests that initiation is inefficient and that only a few sites rapidly propagate, in agreement with reports of other initiator systems containing  $\pi$ -allyl ligands.<sup>[18]</sup>

A significant increase in reactivity was observed in the presence of  $\text{Al}(\text{C}_6\text{F}_5)_3$  (Table 1, entries 3–5). The productivity was two orders of magnitude larger with 5 equivalents of the coactivator than with **2** alone. The higher activity observed with 5 equivalents of  $\text{Al}(\text{C}_6\text{F}_5)_3$  than with 1 equivalent may be attributed to the scrubbing of impurities within the reaction medium and/or a shift of the equilibrium towards the adduct. The addition of  $\text{Al}(\text{C}_6\text{F}_5)_3$  also led to a large increase in the molecular weight of the product (from  $M_w \approx 50 \times 10^3 \text{ g mol}^{-1}$  with **2** to  $M_w \approx 1 \times 10^6 \text{ g mol}^{-1}$  with **2**/ $\text{Al}(\text{C}_6\text{F}_5)_3$ ; Table 1, entries 2 and 5). Comparison of the molecular weight of the products and productivities indicate that **2**/ $\text{Al}(\text{C}_6\text{F}_5)_3$  does not initiate the reaction completely at the beginning of the polymerization. An increase in the amount of the coactivator from 1 to 5 equivalents resulted in an almost threefold increase in the activity (Table 1, entries 3 and 4). An increase in the reaction temperature to  $75^\circ\text{C}$  under these conditions resulted in a large increase in ethylene consumption and an average productivity of 4800 kg of PE per mol of Ni per hour (Table 1, entry 5), which corresponds to an apparent turnover frequency (TOF) of  $1.7 \times 10^5 \text{ h}^{-1}$ . The molecular-weight distribution of the polymer in entry 5 of Table 1 is broadened. We attribute this effect to inefficient initiation, limitation to short reaction times, and gelation of the reaction medium as a result of the rapid production of high-molecular-weight PE. However, the activity observed for the reaction in entry 5 of Table 1 is comparable to that observed with the **1**/MAO combination.

The reactivity of **4** and **5** was lower than that observed with **2**/ $\text{Al}(\text{C}_6\text{F}_5)_3$  (Table 1, entries 6 and 7). These observations may bear implications for why it is important to remove TMA from MAO to achieve living-polymerization conditions. Specifically, the formation of analogues of **4** by reaction with TMA would increase and modify the diversity of propagating

**Table 1:** Selected ethylene-polymerization reactions.<sup>[a]</sup>

Entry	Initiator	Coactivator (equiv)	<i>t</i> [min]	<i>T</i> [°C]	Activity <sup>[b]</sup>	$M_w$ [ $10^3 \text{ g mol}^{-1}$ ] <sup>[c]</sup>	$M_w/M_n$ <sup>[d]</sup>	$T_m$ [°C] <sup>[e]</sup>
1	<b>2</b>	–	60	50	20	47	1.9	128
2	<b>2</b>	–	20	75	73	51	6.6	118
3	<b>2</b>	$\text{Al}(\text{C}_6\text{F}_5)_3$ (1)	20	50	300	1088	4.3	125
4	<b>2</b>	$\text{Al}(\text{C}_6\text{F}_5)_3$ (5)	20	50	800	836	3.5	121
5	<b>2</b>	$\text{Al}(\text{C}_6\text{F}_5)_3$ (5)	10	75	4800	1050	bimodal	118
6	<b>4</b>	–	20	50	15	180	2.1	131
7	<b>4</b>	–	20	50	70	295	2.6	124

[a] Polymerizations were carried out in a 300 mL autoclave reactor in toluene (50 mL) with 10  $\mu\text{mol}$  of the complex at an ethylene pressure of 500 psig. [b] The activity is given in kg of PE per mol of Ni per hour. [c] The weight-average molecular weight of the product was determined by gel-permeation chromatography versus polystyrene standards. [d]  $M_n$  = number-average molecular weight. [e] The melting temperature of the product was determined by differential scanning calorimetry.

sites during the timescale of polymerization and limit control over the PE structure. The addition of up to 5 equivalents of TMA (for **4**) or TEA (for **5**) did not lead to appreciable increases in activity.

In conclusion, we have described the synthesis and characterization of the discrete, cationic nickel complex **2**, which offers insight into the propagating sites generated by using **1** in the presence of various coactivators. Multinuclear NMR spectroscopy is consistent with the addition of Al( $C_6F_5$ )<sub>3</sub> to the carbonyl site in **2** to form the cationic complex **3**, the electron density of which is further depleted. Al( $C_6F_5$ )<sub>3</sub> binding also leads to an increase in reactivity towards ethylene and in the molecular weight of the polymer products. These observations are fully consistent with the originally proposed active site shown in Scheme 1. From a practical perspective, thermally robust polymerization sites can be generated without the use of large excesses of aluminum reagents. The reaction of **2** with TMA commonly present in MAO solutions results in Al–C addition across the carbonyl functionality and rearrangement of the ligand framework to give the binuclear organometallic species **4**. The reaction with TEA proceeds by a more complex mechanism, but the final product is complex **5**, which is closely related to **4**. The formation of **4** and **5** indicates that the carbonyl group in the  $\alpha$ -keto- $\beta$ -diimine not only serves as a conduit for modification of the electron density at the metal, but can also participate in deactivation reactions that must be carefully mitigated to ensure maximum control over the product properties.

Received: May 24, 2010

Revised: July 14, 2010

Published online: August 25, 2010

**Keywords:** cationic complexes · homogeneous catalysis · nickel · polymerization · polyolefins

- [1] a) W. Kaminsky, *Macromol. Chem. Phys.* **2008**, *209*, 459–466; b) B. Rieger, L. Baugh, S. Striegler, S. Kacker, *Late Transition Metal Polymerization Catalysis*, Wiley, New York, **2003**; c) R. Blom, A. Follestad, E. Rytter, M. Tilset, M. Ystenes, *Organometallic Catalysts and Olefin Polymerization: Catalysts for a New Millennium*, Springer, Berlin, **2001**; d) L. K. Johnson, S. Mecking, M. Brookhart, *J. Am. Chem. Soc.* **1996**, *118*, 267–268; e) S. Mecking, L. K. Johnson, L. Wang, M. Brookhart, *J. Am. Chem. Soc.* **1998**, *120*, 888–899; f) T. R. Younkin, E. F. Connor, J. I. Henderson, S. K. Friedrich, R. H. Grubbs, D. A. Bansleben, *Science* **2000**, *287*, 460–462; g) S. D. Ittel, L. K. Johnson, M. Brookhart, *Chem. Rev.* **2000**, *100*, 1169–1203; h) A. Berkefeld, S. Mecking, *Angew. Chem.* **2008**, *120*, 2572–2576; *Angew. Chem. Int. Ed.* **2008**, *47*, 2538–2542.
- [2] a) Z. Guan, P. M. Cotts, E. F. McCord, S. J. McLain, *Science* **1999**, *283*, 2059–2062; b) M. D. Leatherman, S. A. Svedja, L. K. Johnson, M. Brookhart, *J. Am. Chem. Soc.* **2003**, *125*, 3068–3081; c) D. Meinhard, M. Wegner, G. Kipiani, A. Hearley, P. Reuter, S. Fischer, O. Marti, B. Rieger, *J. Am. Chem. Soc.* **2007**, *129*, 9182–9191.
- [3] a) C. M. Killian, D. J. Tempel, L. K. Johnson, M. Brookhart, *J. Am. Chem. Soc.* **1996**, *118*, 11664–11665; b) A. C. Gottfried, M. Brookhart, *Macromolecules* **2001**, *34*, 1140–1142; c) J. D. Azoulay, Y. Schneider, G. B. Galland, G. C. Bazan, *Chem. Commun.* **2009**, 6177–6179.
- [4] a) S. J. McLain, K. J. Sweetman, L. K. Johnson, E. F. McCord, *Polym. Mater. Sci. Eng.* **2002**, *86*, 320–321; b) C. S. Propeny, D. H. Camacho, Z. Guan, *J. Am. Chem. Soc.* **2007**, *129*, 10062–10063; c) S. J. Diamanti, P. Ghosh, F. Shimizu, G. C. Bazan, *Macromolecules* **2003**, *36*, 9731–9735.
- [5] a) A. Held, F. M. Bauers, S. Mecking, S. K. Friedrich, *Chem. Commun.* **2000**, 301–302; b) F. M. Bauers, S. Mecking, *Macromolecules* **2001**, *34*, 1165–1171; c) B. Korthals, I. G. Schnetmann, S. Mecking, *Organometallics* **2007**, *26*, 1311–1316.
- [6] a) A. Nakamura, S. Ito, K. Nozaki, *Chem. Rev.* **2009**, *109*, 5215–5244; b) B. M. Boardman, G. C. Bazan, *Acc. Chem. Res.* **2009**, *42*, 1597–1606.
- [7] a) L. K. Johnson, C. M. Killian, M. Brookhart, *J. Am. Chem. Soc.* **1995**, *117*, 6414–6415; b) S. A. Svedja, L. K. Johnson, M. Brookhart, *J. Am. Chem. Soc.* **1999**, *121*, 10634–10635.
- [8] a) B. Y. Lee, G. C. Bazan, J. Vela, Z. J. A. Komon, X. Bu, *J. Am. Chem. Soc.* **2001**, *123*, 5352–5353; b) Z. J. A. Komon, X. Bu, G. C. Bazan, *J. Am. Chem. Soc.* **2000**, *122*, 1830–1831; c) Y. H. Kim, T. H. Kim, B. Y. Lee, *Organometallics* **2002**, *21*, 3082–3084.
- [9] J. D. Azoulay, R. S. Rojas, A. V. Serrano, H. Ohtaki, G. B. Galland, G. C. Bazan, *Angew. Chem.* **2009**, *121*, 1109–1112; *Angew. Chem. Int. Ed.* **2009**, *48*, 1089–1092.
- [10] MMAO, a modified methylaluminoxane activator containing 25% isobutylaluminoxane, is prepared by the controlled hydrolysis of trimethylaluminum and triisobutylaluminum.
- [11] J. Feldman, S. J. McClain, A. Parthasarathy, W. J. Marshall, J. C. Calabrese, S. D. Arthur, *Organometallics* **1997**, *16*, 1514–1516.
- [12] a) E. Y.-X. Chen, T. J. Marks, *Chem. Rev.* **2000**, *100*, 1391–1434; b) J. Tian, D. Hustad, G. W. Coates, *J. Am. Chem. Soc.* **2001**, *123*, 5134–5135; c) M. Mitani, R. Furuyama, J.-I. Mohri, J. Saito, S.-I. Ishii, H. Terao, N. Kashiwa, T. Fujita, *J. Am. Chem. Soc.* **2002**, *124*, 7888–7889; d) T. Hasan, A. Ioku, K. Nishii, T. Shiono, T. Ikeda, *Macromolecules* **2001**, *34*, 3142–3145; e) V. Busico, R. Cipullo, F. Cutillo, N. Friederichs, S. Ronca, B. Wang, *J. Am. Chem. Soc.* **2003**, *125*, 12402–12403.
- [13] K. Landolsi, M. Rzaigui, F. Bouachir, *Tetrahedron Lett.* **2002**, *43*, 9463–9466.
- [14] S. Feng, G. R. Roof, E. Y.-X. Chen, *Organometallics* **2002**, *21*, 832–839.
- [15] D. Chakraborty, E. Y.-X. Chen, *Organometallics* **2003**, *22*, 207–210.
- [16] a) E. C. Ashby, J. T. Laemmle, *Chem. Rev.* **1975**, *75*, 521–546; b) S. Dagorne, D. Atwood, *Chem. Rev.* **2008**, *108*, 4037–4069.
- [17] A. Corma, G. Hermenegildo, *Chem. Rev.* **2002**, *102*, 3837–3892.
- [18] W. Liu, J. M. Malinoski, M. Brookhart, *Organometallics* **2002**, *21*, 2836–2838.
- [19] Crystal data for **2**:  $C_{131.5}H_{121}B_2C_{13}F_{48}N_4Ni_2O_2$ ,  $M_r = 2946.71$ , triclinic, space group  $P\bar{1}$ ,  $a = 18.798(5)$ ,  $b = 18.977(6)$ ,  $c = 20.160(6)$  Å,  $\alpha = 78.460(5)$ ,  $\beta = 80.121(5)$ ,  $\gamma = 72.287(6)^\circ$ ,  $V = 6653(3)$  Å<sup>3</sup>,  $Z = 2$ , red, crystal size  $0.3 \times 0.25 \times 0.2$  mm<sup>3</sup>,  $Mo_{K\alpha}$ ,  $\lambda = 0.71073$  Å,  $T = 150(2)$  K,  $R = 7.51$ ,  $wR = 16.69$  for 26345 unique reflections with  $I > 2\sigma(I)$ . Crystal data for **4**:  $C_{71.5}H_{69}AlBF_4N_2NiO$ ,  $M_r = 1524.79$ , monoclinic, space group  $P2_1/c$ ,  $a = 18.788(3)$ ,  $b = 19.309(4)$ ,  $c = 21.682(4)$  Å,  $\beta = 103.596(3)^\circ$ ,  $V = 7645(2)$  Å<sup>3</sup>,  $Z = 4$ , yellow, crystal size  $0.35 \times 0.3 \times 0.08$  mm<sup>3</sup>,  $Mo_{K\alpha}$ ,  $\lambda = 0.71073$  Å,  $T = 150(2)$  K,  $R = 8.18$ ,  $wR = 20.70$  for 26345 unique reflections with  $I > 2\sigma(I)$ . Crystal data for **5**:  $C_{69}H_{69}AlBF_4N_2NiO$ ,  $M_r = 1494.76$ , triclinic, space group  $P\bar{1}$ ,  $a = 12.801(4)$ ,  $b = 14.565(5)$ ,  $c = 20.084(7)$  Å,  $\alpha = 84.322(5)$ ,  $\beta = 72.372(5)$ ,  $\gamma = 87.243(6)^\circ$ ,  $V = 3551(2)$  Å<sup>3</sup>,  $Z = 2$ , yellow, crystal size  $0.3 \times 0.25 \times 0.25$  mm<sup>3</sup>,  $Mo_{K\alpha}$ ,  $\lambda = 0.71073$  Å,  $T = 150(2)$  K,  $R = 7.86$ ,  $wR = 16.72$  for 13875 unique reflections with  $I > 2\sigma(I)$ . CCDC 777724 (**2**), 777723 (**4**), and 777722 (**5**) contain the supplementary crystallographic data for this paper. These data can be obtained free of charge from The Cambridge Crystallographic Data Centre via [www.ccdc.cam.ac.uk/data\\_request/cif](http://www.ccdc.cam.ac.uk/data_request/cif).